A New Green Coating for the Protection of Frescoes: From the Synthesis to the Performances Evaluation

Raffaella Lamuraglia [1,2], Andrea Campostrini [1], Elena Ghedini [1], Alessandra De Lorenzi Pezzolo [3], Alessandro Di Michele [4], Giulia Franceschin [2], Federica Menegazzo [1,2,*], Michela Signoretto [1] and Arianna Traviglia [2]

1   CATMAT Lab, Dipartimento di Scienze Molecolari e Nanosistemi, Università Ca' Foscari Veneziaand INSTM RUVe, 30170 Venice, Italy
2   Center for Cultural Heritage Technology, Istituto Italiano di Tecnologia, 30170 Venice, Italy
3   Dipartimento di Scienze Molecolari e Nanosistemi, Università Ca' Foscari Venezia, 30170 Venice, Italy
4   Dipartimento di Fisica e Geologia, Università di Perugia, 06123 Perugia, Italy
*   Correspondence: fmenegaz@unive.it

Abstract: This work presents the formulation and characterization of a new product for the protection of outdoor frescoes from aggressive environmental agents. The formulation is designed as an innovative green coating, prepared through a zero-waste one-pot-synthetic method to form silver nanoparticles (AgNPs) directly in a chitosan-based medium. The AgNPs are seeded and grown in a mixed hydrogel of chitosan, azelaic, and lactic acid, by the reduction of silver nitrate, and using calcium hydroxide as precipitating agent. The rheological properties of this coating base are optimized by the addition of a solvent mixture of glycerol and ethanol with a 1:1 volume ratio. The new formulation and two commercial products (Paraloid® B72 and Proconsol®) are then applied by brush to ad hoc mock-ups to be evaluated for chemical stability, color and gloss variations, morphological variation, hydrophobicity, and water vapor permeability via Fourier-transform infrared spectroscopy (FT-IR) in attenuated total reflection (ATR) mode, spectrophotometer analysis, stereomicroscope observations, UNI EN 15802, and UNI EN 15803, respectively. The results show that the application of the hybrid chitosan-AgNPs coating is promising for the protection of outdoor frescoes and that it can underpin the development of new products that address the lack of conservation strategies specifically designed for wall painting.

Keywords: green coating; chitosan; AgNPs; frescoes; zero-waste one-pot synthesis

1. Introduction

Historical buildings, open-air mural paintings, and monuments located outdoors are constantly exposed to many different degradation factors i.e., humidity, ultraviolet (UV) light, pollution, microbiological colonization, whose effects may be exacerbated by the influence of climate changes [1–4]. The degradation processes can impact both the bulk and the surface of materials [5–7]. The decorated surface of mural paintings represents the layer in which the exchange of pollutants and water from the environment occurs predominantly, and, thus, is the part that is most susceptible to alteration of its material properties [8]. Water and other water-related decay mechanisms—such as crystallization of insoluble salts, erosion, and pollutant deposition—are described in the literature as the most impactful degradation phenomena for mural paintings. Acting together, these mechanisms are responsible for triggering other severe decay forms, such as biological colonization, detachments, or even more complex characteristic phenomena such as *flos tectori* [9].

Most of the conservation practices currently adopted to preserve wall-painting exposed to not-controlled environments, however, are limited to physical barriers meant to decrease the impact of damaging environmental agents such as rain (e.g., external structures such

as roofing and canopies, as seen in Pompeii, Herculaneum, or Malta), resulting in limited protection and in the persistence of adverse micro-climate conditions [10–12].

Despite several documented forms of degradation, specific products for the in situ protection of frescoes are not commercially available, and even research on this particular type of material is still scarce. Restorers often address this lack of product by using materials that were originally designed for other applications (for instance, products for consolidation and generic fixing of common stone materials) and often ignore the long-term effects of these compounds on delicate systems such as frescoes. In most cases, they are applied with the main purpose of restoring the bulk of the wall rather than the surface layer. Three classes of treatments for fresco restoration can currently be identified on the market according to their properties as either consolidant, filler, or adhesive. Some of the most employed products are consolidants, made of organic or inorganic polymers, nanomaterials, and bio-consolidants, with generic adhesive, cohesive, and film-forming properties [13]. Their own chemical nature is key to their poly-functionality. A common example is Proconsol® (Casoria Arpino, Italy), which is a commercial product sold as a protective and consolidant solution of calcium hydroxide ($Ca(OH)_2$) specifically for wall-painting and frescoes by the Cimmino Calce company [14]. Paraloid® B72 (C.T.S. s.r.l., Altavilla Vicentina, Italy), an ethyl-methacrylate copolymer, is another example and one of the most popular products used by restorers for different kinds of applications, including wall and stone material protection and consolidation [15].

New products designed for Cultural Heritage applications must meet the requirements imposed by the Restoration Charters, which prescribe them to be as compatible as possible with the material on which they are applied, so that they do not modify the external appearance of the treated surface [16]. Protective coatings can be designed to completely embrace this concept and, for this reason, in the last decades, they have gained increasing interest within the scientific community. In fact, while complying with the widely accepted 'gold standards' of restoration, they also meet additional, relevant requirements: transparency, reversibility or re-treatability, compatibility with the surface, long-term lifetime, ease of synthesis, low-cost maintenance, and non-toxicity [17,18]. In addition, particular attention should be placed on developing products that comply with green principles and are risk-free for conservators, restorers, and the environment [18]. The discussion around the feasibility and opportunity of some of these requirements, however, is still ongoing: Andreotti et al. (2018), for example, have argued that achieving the full reversibility of treatments is often just an idealistic goal and that a more viable method could be that of retreating the surfaces [19]. Biopolymers and waste-derived materials are considered as valid alternatives to synthetic ones. The increasing interest in bio-polymers is due to the fact that they naturally comply to the principles of reversibility and/or re-treatability: the polymer is expected to disappear from the surface once its water-repellent properties disappear without affecting subsequent conservative treatments [19]. In recent studies [19–21], biopolymers, such as zein, pectin, chitosan, polyhydroxybutyrate (PHB), and poly-l-lactic acid (PLA), were employed to replace synthetic polymers in many applications, with appreciable results [22]. Among biopolymers, chitosan was estimated to be particularly promising due to its biodegradability, biocompatibility, and antimicrobial activity; therefore, it has recently been used for the formulation of sustainable coatings as an anti-corrosion coating for indoor bronze metal substrates [23,24]. Chitosan, which derives from the partial deacetylation of chitin [25], is considered as a non-toxic biopolymer for its excellent antimicrobial and antifungal activities against a wide range of microorganisms when compared to other polymers and biopolymers [26,27]. Xin Wang et al. successfully designed and developed a controlled release-system against microorganisms based on thymol-loaded chitosan nanoparticles, demonstrating that it is possible to obtain natural biocides as a viable alternative to the toxic products currently in use for the same purpose [28]. Another example of the application of chitosan based on its physical and antimicrobial characteristics is the treatment of ethnographic objects (made of cotton and linen) by L. Indrie et al. [29]. Notwithstanding this potential for threating several types

of cultural heritage, however, chitosan has not been tested yet on frescoes to the best of our knowledge.

Nanoparticles are another important element in the formulation of protective coatings, because of their ability to add specific physical and chemical properties to the resulting film. Among others, even silver nanoparticles (AgNPs) have attracted more and more attention in different research fields due to their potential as antimicrobial agents [30]. The antimicrobial behavior of silver is enhanced when the material is organized in the form of NPs, thanks to the electronic effect given by the changes in the local electronic order on the surfaces of objects with an average size <100 nm. The antimicrobial property of AgNPs could be enhanced in hybrid formulation with polysaccharides due to plasmonic resonance effects, eventually inducing photocatalytic phenomena [31–33].

Based on the above, the authors have selected chitosan as the most appropriate element to underpin the formulation of an innovative organic–inorganic hybrid system to be applied to frescoes and a porous matrix of chitosan hosting Ag active nanoparticles which has been created through a novel one-pot synthesis method. As inorganically charged, AgNPs are grown in-situ in the synthesis medium using a one-pot process, starting from silver nitrate as a precursor. The novelty of this work is represented by the synthesis method, which consists of growing AgNPs within the chitosan-based hybrid matrix prepared using azelaic and lactic acid instead of acetic acid, while the hybrid matrix acts as a reducing, capping, and stabilizing agent simultaneously. Both acetic and azelaic acid are green compounds; however, the latter presents intrinsic antimicrobial features which are able to prevent biological attacks on a treated surface. Furthermore, azelaic acid has a long chain structure that enhances its film-forming ability. Azelaic acid combined with lactic acid can effectively hydrolyze chitosan to exert its reducing and capping action. The resulting hybrid material is the core of the product, and it will be reported in this work as coating base. To optimize the rheological properties of the final product and obtain a ready-to-use formulation which easily applicable by brush and in situ, the coating base is mixed with suitable solvents (i.e., glycerol and ethanol), selected for their own affinity with the coating base and their own rheological properties.

To validate the protective features of the proposed coating, the final properties are compared with those of two commercial products, i.e., Paraloid® B72 (C.T.S. s.r.l., Altavilla Vicentina, Italy) and Proconsol® (Casoria Arpino, Italy). The analyses are carried out on both the coatings and the treated surfaces of fresco mock-ups.

2. Materials and Methods

2.1. Preparation of Chitosan and AgNPs Coating Base

Chitosan (CAS 9012-76-4), azelaic acid (CAS 123-99-9), lactic acid (CAS 50-21-5), and sodium hydroxide (CAS 1310-73-2) were purchased from Sigma-Aldrich® (Merck Life Science S.r.l., Milan, Italy), and silver nitrate (CAS 7761-38-8) and calcium hydroxide (CAS 1305-62-0) were purchased from Acros Organics, (Fisher Scientific, Thermo Fisher Scientific, Waltham, MA, USA). Both are used for the synthesis.

A chitosan-based medium (Medium Molecular weight) is prepared by adding the appropriate amount of reagents, as reported in Table 1, to 15 mL of deionized water.

Table 1. Amount of reagents used for the coating base's synthesis.

Reagent	Quantity
Chitosan	30 mg
Azelaic Acid	9.5 mg
Lactic Acid	300 μL (5% *v/v*)

Silver NPs are synthesized in-situ in a one-pot synthesis together with chitosan, as suggested by Goy, R.C., et al. (2009) [26]. Different concentrations (0.5 M, 0.1 M, and 0.01 M) of silver nitrate in water are investigated as AgNPs precursor. The effects of AgNPs precipitation are tested in a solution of NaOH 0.3 M, as normally done in the

literature [27], and in a 0.015 M solution of Ca(OH)$_2$. The beaker containing the gel is aged at 95 °C for 4 h with constant stirring at 300–400 rpm. The hydro-gel color changes after the first hour, turning to intense yellow/orange/brown after the fourth hour, indicating AgNPs formation.

2.2. Addition of Solvents

Glycerol (CAS 56-81-5) and ethanol (CAS 64-17-5) purchased from Sigma-Aldrich® (Merck Life Science S.r.l., Milan, Italy) are used as solvents without further purification. The two solvents are mixed in a proportion of 1:1. The final formulation is prepared by blending in, at a proportion of 1:1, the coating-base with the solvents mixture.

Once the new coating is ready to be applied, the fresco mock-ups are treated with it and with the commercial products Proconsol® (Casoria Arpino, Italy) and Paraloid B72® (C.T.S. s.r.l., Altavilla Vicentina, Italy) using a brush to compare and validate the protective features of the newly formulated coating (0.6 L m^{-2} applied by brush).

2.3. Mock-Ups Preparation

Sixteen bricks of 5 cm × 5 cm × 2.5 cm are prepared to replicate the characteristics of original fresco samples, following the recipe reported by Vitruvius in *De Architectura*. After 12 h immersion in water, three/four parallel grooves are dug with a 10 mm-diameter drill on each mock-up, to simulate the wall inhomogeneity and to enhance the plaster grip on the material.

To obtain a wider perspective, the *arriccio* layer is prepared using slaked lime (C.T.S. s.r.l., Altavilla Vicentina, Vicenza, Italy) and three different inert materials: *cocciopesto*, *pozzolana*, and white river sand (all purchased from C.T.S. s.r.l., Altavilla Vicentina, Vicenza, Italy). Three plaster doughs are prepared using a proportion of 3:2 between inert material and slaked lime. The first inert material (sand-based) is prepared mixing at a proportion of 1:2 coarse and thin-grained white river sand. The second (*cocciopesto*-based) and the third (*pozzolana*-based) inert materials are prepared by mixing, at a proportion of 1:1:1, coarse-grained sand, thin-grained white river sand, and *cocciopesto* or *pozzolana* powder, respectively.

The bricks with the *arriccio* layer are then dried for approximately 16 h in air. Afterwards, the surface is moistened with water, by means of a sponge float, in order to apply the thinner *intonachino* layer. The *intonachino* is prepared with slaked lime and thin-grained white river sand (in proportion 1:1), on which the pigments (yellow ochre #40301 and red ochre #48651 purchased from Kremer Pigmente GmbH & Co. KG, DE 88317, Aichstetten) are dispersed in water and applied by brush.

2.4. Benchmark Products Selected and Tested

Proconsol® and ParaloidB72® are tested as reference benchmark products. Proconsol® (water dispersion of Ca(OH)$_2$) was kindly provided by Cimmino Calce s.r.l., Casoria Arpino, Naples, Italy. To date, it is the only commercially-available product sold as protective coating for frescoes. The product is applied without further dilution. ParaloidB72® (C.T.S. s.r.l., Altavilla Vicentina, Vicenza, Italy), an ethyl-methacrylate copolymer, is diluted at 5% (*w/v*) in ethyl acetate (CAS 141-78-6, purchased from Sigma-Aldrich®, Merck Life Science S.r.l., Milan, Italy). It is one of the most common benchmark products used by restorers for wall and stone material protection and consolidation.

2.5. Characterization Techniques for Coating

To identify the optimal formulation parameters, UV spectroscopy, Scanning Electron Microscopy, and Transmission Electron Microscopy analyses are carried out. Rheology analyses are run to measure the viscosity of the different coatings.

A UV-Vis spectrophotometer Cary300 by Agilent technologies is used for the analyses. The spectra are collected in the 800–200 nm wavelength range. The analyses are run

through the Cary WinUV Scan software 4.20 and processed with the software Origin 2021 by OriginLab, Northampton, MA, USA.

The SEM microscopy analyses on the different NP samples are carried out by an FE-SEM (Field Emission Scanning Electron Microscopy) FEG LEO 1525 ZEISS, with detector in-lens for secondary electrons. The acceleration potential voltage is maintained at 15 keV and measurements are carried out using an AsB detector (Angle selective Backscattered detector). Samples are deposited on a silicon wafer, dried in air, and observed without metallization.

TEM images are obtained using a Philips 208 Transmission Electron Microscope. The samples are prepared by putting one drop of AgNPs solution on a copper grid pre-coated with a Formvar film and dried in air.

The rheology analyses are run to measure the viscosity of the different coatings. For each sample, around 5 mL is poured into the rheometer cylindrical cup (approx. volume of 19 mL and radius of 14.452 mm). The instrument used for these analyses is a Modular Compact Rheometer (MCR 102) from Anton Paar GmbH, with a No. 3912 coaxial cylinder measuring system. A measuring Bob with radius of 13.331 mm, Ratio of Radii of 1.084, and Gap Length of 39.998 mm is employed. The cone angle is 120° and the measuring gap is 1.121 mm. For the time settings, 21 data points are collected with a point duration of 30 s, an interval duration of 630 s, and an averaging over minimum of 1 raw value. The measuring profile is set with a logarithmic shear rate of $d\gamma/dt$ from 10 to 1000 s^{-1}. The data are collected with the RheoCompass software and processed with the software Origin 2021 of OriginLab, Northampton, MA, USA.

2.6. Characterization Techniques for Applied Coatings

Before and after the ageing process, the mock-ups are characterized to evaluate the physical and chemical properties using ATR spectroscopy, measures of the color variance (ΔE), and the surface gloss, by stereomicroscopic investigation of the morphology and by evaluating the surface hydrophobicity through the contact angle measure.

The measurements are carried out using a VERTEX 70 v FT-IR Spectrometer (Bruker, Billerica, MA, USA) equipped with a PIKE MIRacle™ universal ATR sampling accessory with a diamond/ZnSe internal reflection element. The spectra are collected in the 4000–650 cm^{-1} spectral range with a 2 cm^{-1} resolution. Two hundred scans are averaged in each run and subjected to Norton Beer (medium) apodisation before Fourier transformation. The obtained spectra are min-max normalized and automatic-baseline corrected with OMNIC Atlus Software 6.0.

The morphological analyses are performed by taking pictures of each mock-up at 1× and 2× magnification by means of a NYKON stereomicroscope model SMZ 745T (European Headquarters Nikon Europe BV, Tripolis 100, Burgerweeshuispad 101, 1076 ER Amsterdam, Netherlands).

Color variations are measured with a Konica Minolta CM 700d spectrophotometer before and after ageing, as well as before and after coating application. The instrument has an 8-degree viewing angle geometry, with a diffusion light Xenon lamp and a high-resolution monolithic polychromator. The analyzed area is circular, with a 3-mm diameter, and the results are obtained by averaging six measurements carried out on different points over the mock-up.

Measurements are performed in the CIELAB1976 space. Results are elaborated by Spectra Magic NX 6. The total color variation, expressed as ΔE, is calculated by Equation (1):

$$\Delta E = \sqrt{[(\Delta L^*)^2 + (\Delta a^*)^2 + (\Delta b^*)^2]}, \tag{1}$$

where ΔL*, Δa*, and Δb* are the differences between the values obtained on the same sample before and after each step. In the Heritage Science field, it is assumed that, when the ΔE values are higher than 3, the chromatic difference is visibly detectable to the naked eye [34–37].

Hydrophobicity tests are done following the UNI EN 15802 document [38], by measuring the contact angle which a water drop makes on the surface of the fresco mock-ups. The procedure is filmed with a Canon camera, mounted with a Canon macro lens of 100 mm.

The water vapor permeability is measured on fresco mock-ups following the steps described in the UNI EN 15803 document [39].

2.7. Ageing Parameters

The fresco mock-ups are artificially aged, before and after the application of the coatings, in a Q-Sun Xe-1S climatic chamber (Q-LAB Corporation, Westlake, OH 44145-1419 SUA) for a total of 72 h to study the effect of temperature, light, and humidity fluctuations. The ageing parameters adopted are the following: 12 h UV-light step with 65 W m^{-2} radiance, T = 50 °C, and 5 s water spray every 4 h (p = 1.4 L min^{-1}), alternated with 12-h dark step with T = 25 °C and 5 s water spray every 4 h (p = 1.4 L min^{-1}). Twenty-four-hour runs composed by 30 min cycles are repeated three times. Between each repetition, the positions of the samples are swapped to ensure that the artificial ageing process homogeneously impacts all of the mock-ups.

3. Results and Discussion

3.1. Coating Base Formulation and Characterization

The comparison of the UV spectra of the different NPs formulations is shown in Figure 1, where all are prepared in azelaic and lactic acid with NaOH, only varying the AgNO$_3$ concentration.
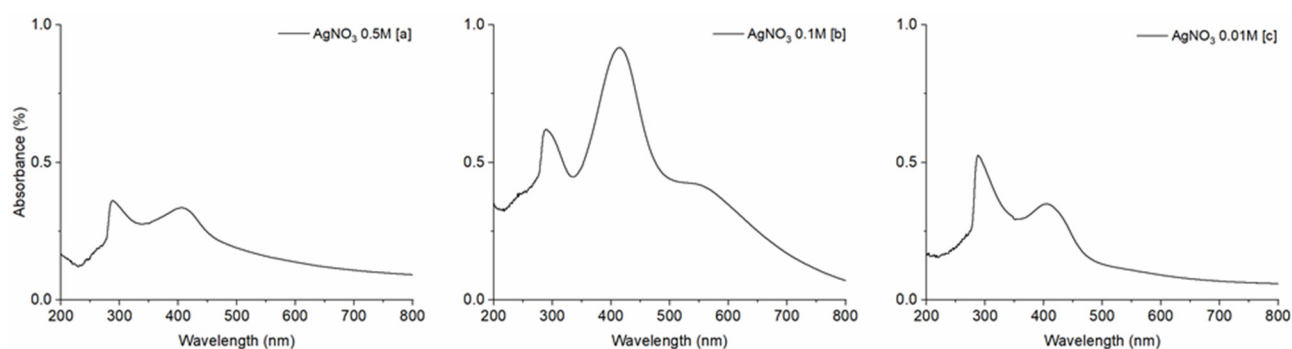

Figure 1. UV-Vis spectra of AgNPS in azelaic and lactic acid solution, with NaOH as precipitating agent. (**a**) AgNO$_3$ 0.5 M, (**b**) 0.1 M, and (**c**) 0.01 M.

UV spectroscopy is useful to study the plasmonic resonance bands of the components present in different coating base samples. The resonance bands at 410 nm are related to the presence of small silver nanoparticles [40]. In the proposed synthesis process, chitosan constitutes the capping and reducing agent: the availability of functional groups such as carboxyl, hydroxyl, and amine determine the number of available nucleation centers and, consequently, the amount of AgNPs, regardless of the precursor concentration. Moreover, when using AgNO$_3$ 0.1 M, another resonance band around 600 nm appears, indicating metal particles with larger dimensions and suggesting a double distribution of the NPs. The resonance bands at 300 nm are due to the presence of unreacted chitosan. Since the solution with AgNPs synthesized by AgNO$_3$ 0.5 M sutures the analysis, the sample is diluted 3:1 with water. As reagent for the precipitation of the NPs, a solution of Sodium Hydroxide (NaOH), as normally used the in literature, and one of Calcium Hydroxide Ca(OH)$_2$, which may increase the compatibility in the application on calcium carbonate-based materials, are tested. The hydroxides are involved in the reduction process by the formation of an Ag(OH)x intermediate with subsequent reduction in silver in an aqueous environment [41]. UV-Vis analyses show that AgNPs are successfully developed when also employing Ca(OH)$_2$. Since the frescoes' bases are principally made of CaCO$_3$, produced by the carbonatation of Ca(OH)$_2$, the addition of Ca(OH)$_2$ would not lead to any unwanted

chemical reaction. For this reason, $Ca(OH)_2$ is chosen as the reagent for the precipitation of the silver nanoparticles. Figure 2 presents the UV spectra of two samples, both prepared with azelaic acid and $AgNO_3$ 0.1 M, employing the two different precipitating agents. In the sample with NaOH, the % absorbance of the band at around 410 nm is higher, which can be correlated with a higher concentration of nanoparticles in the final product. In addition, the presence of $Ca(OH)_2$ seems to enhance the phenomenon of the double distribution of the nanoparticles' sizes, as shown by the increased intensity of the 600 nm band.
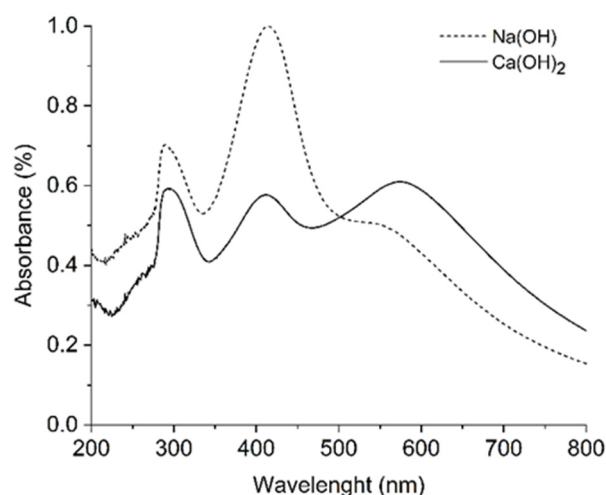

Figure 2. UV-Vis spectra of AgNPs in azelaic and lactic acid solution, with $AgNO_3$ 0.1 M, and NaOH and $Ca(OH)_2$, as precipitating agents.

Thanks to SEM and TEM analyses, it is possible to investigate the silver NPs distributions, shapes, and sizes (Figure 3). SEM images show that all of the samples contain silver NPs homogeneously distributed in the chitosan gel. Thanks to TEM images, it is possible to observe that the NPs are not aggregated, spherical in shape, or nano-dimensional. This allows for confirmation that the sample in which 0.1 M silver nitrate and $Ca(OH)_2$ are used has a double distribution of the NPs sizes.
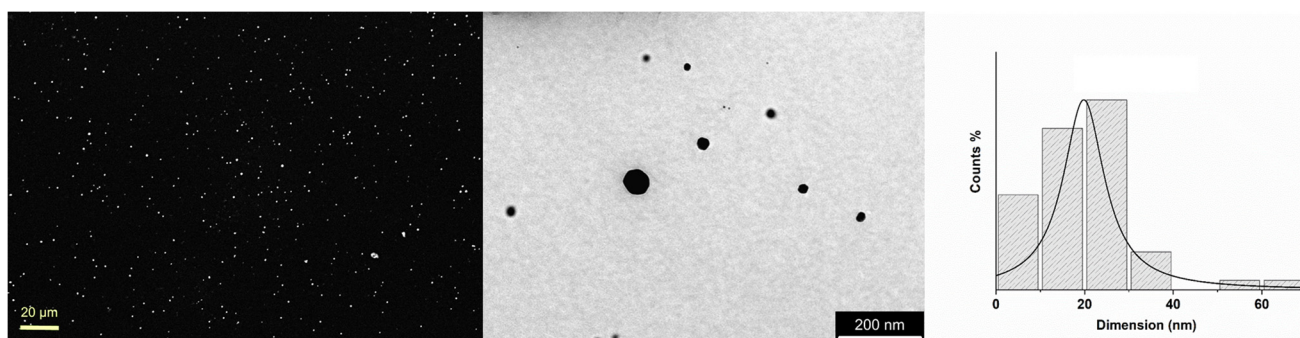

Figure 3. (From left to right) SEM (EHT = 15.00 kV, WD = 7.6 mm, Mag = 1.00 K X, Signal A = AsB), TEM, and distribution curve of AgNPs in lactic and azelaic acid solution, with $AgNO_3$ 0.1 M and $Ca(OH)_2$ as precipitating agent. ImageJ software (LOCI, University of Wisconsin, Madison, WI, USA) is used to estimate the particle size distribution of NPs by TEM images.

To obtain suitable rheological properties, an additional solvent is added to the formulation. The first tests are performed using the same solvents employed in the commercial products for cultural heritage restorations: ethyl acetate ($CH_3COOC_2H_5$) (as in Paraloid®) and water (as in Proconsol®). Other solvents are also taken into account (i.e., glycerol, ethanol, isopropanol), and the product behavior at variable ratios of 1:10 or 1:5 base to solvent is investigated. Ethyl acetate is a moderately-polar solvent that has the advan-

tages of being volatile, relatively non-toxic, and non-hygroscopic. Nevertheless, it is quite unstable in the presence of strong aqueous bases and acids. Water is the best solvent in terms of toxicity, availability, and cost; however, it has low volatility. Glycerol, as well, has all the advantages of water, being non-toxic, easily available, and economic. Ethanol has very high volatility but is still a good solvent for its low toxicity and easy synthesis. Finally, isopropanol has high volatility as well but is also quite toxic. The dilution with ethyl acetate, unfortunately, damages the coating, altering the chitosan matrix stability and producing a white precipitate; therefore, it is excluded. On the contrary, with water, glycerol, ethanol, and isopropanol, no visible damage is encountered, even after two months. The crucial point is to study the nanoparticles' stability in different environments and to achieve a product with medium volatility and an adequate evaporation rate. A solvent with low volatility (as glycerol) delays the evaporation, favoring the coating application, but increasing the risk of leakage. On the other hand, a solvent with excessively-high volatility (such as isopropanol) impedes a homogeneous coating application on the surface. Finally, even if it could be an ideal solvent for applications in Cultural Heritage, its low volatility is a limiting factor that leads to discarding water.

The final coating is prepared by blending the above-described gel in a proportion of 1:1 with a mixture of glycerol and ethanol that combines the properties of the two solvents and reaches a good compromise between volatility and applicability. As expected, the viscosity values obtained for the new formulation and for the commercial products (i.e., Paraloid® and Proconsol®) are different, in line with their different chemical compositions. All the samples present a rheological behavior appropriate to an application by brush: Proconsol® and Paraloid® have an average viscosity value, respectively, of 2 and 3 mPa·s (Table 2), whereas the Chitosan gel with AgNPS showed a higher viscosity (13 mPa·s). This is a promising aspect, which would allow for keeping the chitosan coating on the outer layers without nullifying the properties of the application [42].

Table 2. Viscosity average values for each coating.

Product	Average Viscosity [mPa·s]
Proconsol®	2
Paraloid B72®	3
Chitosan AgNPs product	13

3.2. Coating Application

The ATR spectroscopy analyses, performed before and after ageing, show that the three coatings have good chemical stability. The spectra of the samples coated with Proconsol® (Figure 4a) and with the new chitosan-AgNPs (Figure 4c) show distinctive features of the first two strata (pigment and *intonachino*) underlying the coating films. The absorptions at about 1430–1395, 872 and 712 cm^{-1} (fundamental bands), and 2873, 2512, and 1795 cm^{-1} (overtone and combination bands) are ascribable to the calcite present both in the *intonachino* layer and, as a filler, in the yellow ochre pigment employed in the sample set investigated by ATR-FTIR. The goethite contained in the pigment can be related to a very weak band present in the spectra at 677 cm^{-1}, and possibly to another one, superimposed to one due to quartz, falling at about 800 cm^{-1}. Other characteristic absorptions of quartz, of which the thin-grained aggregate fraction of the *intonachino* layer is made, are found at about 1170, 1085, and 780 cm^{-1}. Signals from amorphous calcite due to the carbonation of the slacked lime are found superimposed to the calcite broad ν_3 band with contributions at about 1395 cm^{-1} and a high-wavenumber shoulder [43], while a very weak peak at 3640 cm^{-1} due to residual Ca(OH)$_2$ can be recognized, indicating an almost complete carbonation. All the spectra show a sharp peak of medium intensity at about 3690 cm^{-1} due to Mg(OH)$_2$, which proves, on the one hand, the presence of a dolomitic component in the commercial slacked lime, and, on the other, the different time scale of the carbonation of magnesium hydroxide process as compared to that of calcium hydroxide [44]. On the

contrary, the two spectra of the Paraloid®-treated samples (Figure 4b) present a quite-different profile where, among the features due to the first two strata below the coating layer of the mock-ups, only the calcium carbonate features at about 875 and 712 cm^{-1} are visible as weak absorptions together with the well-defined sharp peak at about 3690 cm^{-1}, corresponding to magnesium hydroxide. This is indicative of the thickness of the protective layer created by the product.
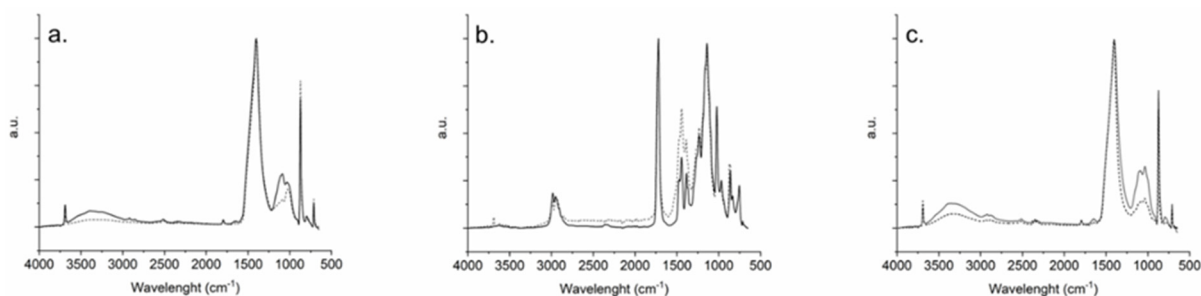

Figure 4. ATR spectra of not-aged (dot-line) and aged Proconsol® (**a**), Paraloid B72® (**b**), and Chitosan AgNPs (**c**).

Overall, the two spectra of the samples treated with Proconsol® do not show any chemical alterations due to degradation phenomena; the variations in the spectral intensity can be attributed, in this case, to a different pressure applied on the diamond cell by the investigated surface. It is unclear, however, due to the Proconsol® formulation, if, in this instance, the weak absorption at 3640 cm^{-1} is related to the product itself or to the calcium hydroxide present in the mock-ups' composition.

ParaloidB72® exhibits good stability over artificial ageing; its main absorption bands present in the two spectra remain basically unchanged and are found at about: 3400–4000 (broad, due to the hydroxyl groups stretching modes), 2988, 2953 (C-H stretching modes), 1725 (ester carbonyl group stretching mode), 1476, 1445 (CH$_3$ asymmetric bending mode), 1387, 1366 (CH$_3$ symmetric bending modes), 1234, 1168, 1140, 1023 (C-C=O-O stretching modes), 968 (C-C stretching mode), 859, 835, and 752 cm^{-1} (C-H rocking modes) [45,46]. Nevertheless, a progressive decrease in all of the main absorptions of the spectrum, and an increase in intensity in the C-H stretching and bending region can be noticed: the first phenomenon could be due to the initial stage of loss of monomers and small fragments formed as a result of the chain scissions, whereas the second one could suggest the beginning of an oxidation process [47–49].

Similarly to the Proconsol®-coated samples, those treated with the new chitosan–AgNPs coating present ATR spectra that reflect the composition of the underlying first two strata and do not display any spectral differences due to degradation, apart from the variations in the spectral intensity. Furthermore, it is possible to identify spectral features that are characteristic of glycerol, present in the formulation, in the region between 1200 and 900 cm^{-1}. Specifically, the signals at about 1039 and 1116 cm^{-1} are attributable to the C-O stretching vibration of the primary and secondary alcohol group, while the band at about 928 cm^{-1} and the small shoulder at 995 cm^{-1} are due to the C-H vibrations [50,51]. After ageing, the bands attributed to glycerol are still present; nevertheless, it is possible to observe an increase in the intensities of the absorptions between 2700 and 3600 cm^{-1}, and changes in band intensities ratios at lower wavenumbers (890 and 1200 cm^{-1} range), due to the curing of the protective layer and the evaporation of the glycerol [52,53]. In particular, the increase in the intensity of the broad band between 3000 and 3600 cm^{-1} is ascribable to the OH-O stretching vibration of the chitosan film; this band grows with the increase of the glycerol content, suggesting a larger number of chitosan-glycerol hydrogen bonds due to the presence of more OH groups provided by the glycerol molecules [52]. The variations in the intensities of the bands at 1036 and 1112 cm^{-1}, and the sharper shape of the spectrum profile in this region, suggest an interaction via hydrogen bonds between

chitosan and glycerol OH groups, as reported by Leceta et al. (2015) [53]. There are no variations in the polymeric fraction of the formulation since the signal does not arise at 1378 cm^{-1} due to chitosan deacetylation, which allows for higher mobility in the polymer and favors a Maillard reaction. Moreover, if there was a structural change in the film as time progressed, a small peak at 986 cm^{-1} should appear [53]. Therefore, it is possible to state that the new formulation based on chitosan is chemically stable within this study and the ageing conditions adopted.

The morphological characterization is pivotal to determining the occurrence of visible degradation or alteration phenomena during the artificial ageing. Moreover, it allows for evaluation of whether the coating's application on the surface altered it or not, and, consequently, its appearance due to a different interaction with light.

The obtained results show that Proconsol® is transparent and very stable over the entire artificial ageing process, and that it does not change the mock-ups' surface morphology, both after its application and after its ageing (Figure S1). On the other hand, after the application of Paraloid B72®, the mock-ups immediately present a shiny/glossy aspect on the surface, which does not decrease after ageing (Figure 5). Lastly, concerning the application of the new product formulated with chitosan gel and silver nanoparticles, the coating seems to be quite stable over time and does not change the surface appearance of the mock-ups on which it was applied, while a slightly white patina is observed after ageing. This phenomenon could be ascribable to the coffee stain effect due to water deposition on the surface during ageing or could be due to salt transport during solvent evaporation, and requires further examination. No crack formation and/or increased roughness is registered due to the degradation of the chitosan polymeric film, induced by UV exposure and temperature fluctuations [54]. However, the morphological observations must be compared with colorimetric data (Figure S2).
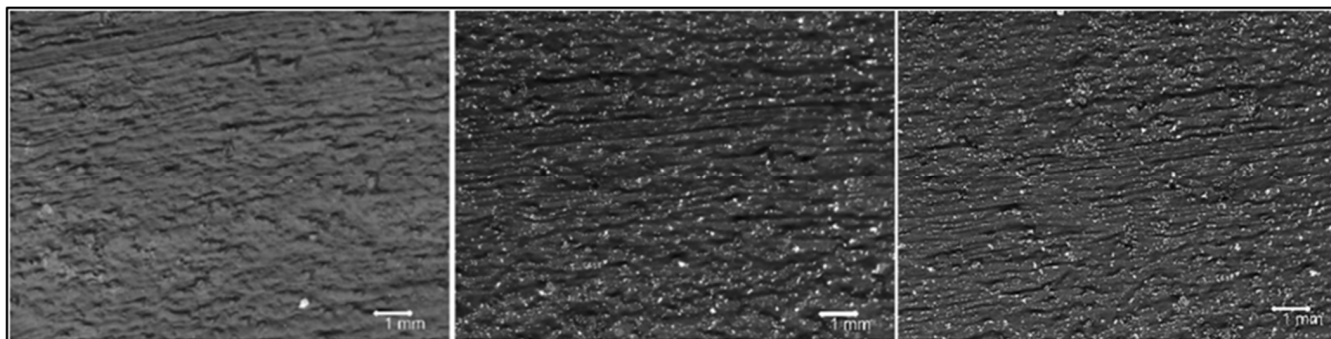

Figure 5. (From left to right) Stereomicroscopy images of untreated, treated with ParaloidB72, and aged with ParalodB72 surfaces.

The colorimetric tests are useful to determine the color variation and the gloss change between before and after the application of the three coatings and to verify if there is any variation after the ageing process. Figure 6 summarizes the ΔE variation of the samples coated with the three products, before (on the left section) and after (on the right section) the artificial ageing process. In the sample treated with Proconsol® (White), the ΔE presents a small variation, lower than 3, and its gloss variation (ΔGloss) is, on average, equal to 0. This means that the Proconsol® coating positively passes the colorimetric test, after the artificial ageing procedure as well. On the contrary, the ΔE variation graph of Paraloid B72® (dark Grey) shows that this product reaches the color limit of the human eye detection. This means that the color change is also visible by the naked eye. Nevertheless, it is worth comparing the ΔGloss between before and after applying Paraloid B72®: unlike the other products which have a Δgloss equal to 0, it presents an average gloss of 7 (Figure S3). This glossy characteristic is a main issue for the use of Paraloid B72®, since it radically changes the aesthetical aspect of mock-ups. Finally, the mock-ups coated with chitosan and silver NPs show good colorimetric results: as reported by Bussiere et al., the exposure to UV light

could photo-oxidize the polymeric film, resulting in the yellowing of the treated surface, not registered here (light Grey) [54]. All treated samples are under the limit of detection of the human eye both after the application, and after the artificial ageing cycles.
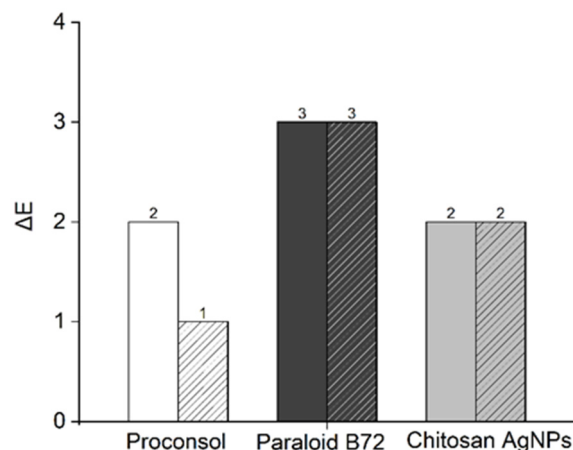

Figure 6. ΔE before (left) and after (right) ageing of the three coatings applied to mock-up surfaces.

Analyses of the contact angle are carried out to investigate the hydrophobicity of the different coatings. As can be seen in Table 3, Proconsol® does not show any sign of increasing the hydrophobicity of the material. This result is a critical aspect in the evaluation of the protective coating features, since water is one of the main degradation factors which affects Cultural Heritage materials exposed outdoors [3], and hydrophobicity is one of the main characteristics required of a superficial coating [55]. Contrarily, Paraloid B72® presents, in all the mock-ups, a higher contact angle, meaning that its application makes the surface more hydrophobic. Its hydrophobicity is also preserved after the artificial ageing process. Likewise, the chitosan gel with silver NPs, even if it has a lower contact angle (51 vs 75 on average), maintains good hydrophobic features over time (only a partially and small loss is observed −13%).

Table 3. Contact angle data of mock-ups coated with Proconsol®, Paraloid B72®, or Chitosan gel.

Contact Angle θ	After the Coating Application	After the Artificial Ageing
Proconsol®	0°	0°
Paraloid B72®	75°	71°
Chitosan AgNPs product	51°	44°

This characterization shows that Paraloid B72® is more effective in making the surface hydrophobic than the formulation presented in this study. Nevertheless, these results must be compared with the ones of the permeability to water vapor (δp) test. This test is crucial to understanding if the product that is being spread on the surface could lead to positive protective interactions or if it would result in a completely impermeable layer over the surface. Since Proconsol® does not present any hydrophobicity, for this test, only Paraloid B72® is taken as a reference product. In Figure 7, it is possible to notice that both tested products, freshly applied and aged, present a lower δp than the uncoated mock-up. However, after ageing, their water vapor permeability increases slightly. These analyses showed that the chitosan-based protective coating is more permeable to water vapor than Paraloid B72®.
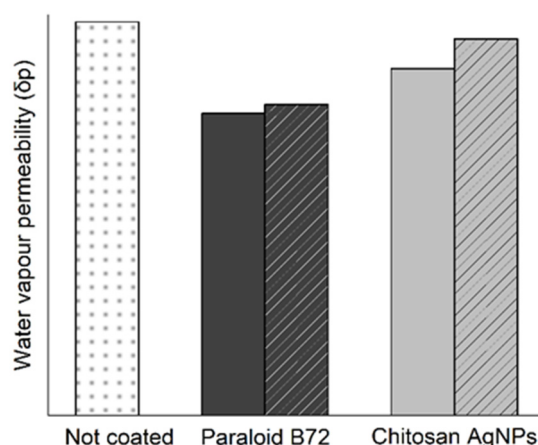
Figure 7. Water vapor permeability of treated mock-ups before (left) and after (right) ageing.

In general, it must be said that the results of all the characterizations proposed in this work do not have to be considered separately, and that only a complete view of the results can lead to appropriate conclusions, correlating the information obtained by the analyses.

3.3. Evaluation of the Coating Performances

To easily evaluate the performances of the investigated coatings, radar charts of six parameters are drawn. For each piece of information (compositional stability, morphology, color variance, gloss variance, hydrophobicity, and permeability to water vapor), a numerical value, on a scale between 0 and 3, is given, where 0 represents unsatisfying results and 3 represents well-performing outcomes. In the adopted evaluation method, assessing the quality of the overall performance, all the parameters are considered as equally important and are all assigned with the same unitary weight. Moreover, it is important to note that the numerical values are assigned based on a purely qualitative assessment by averaging the results obtained both after application and after aging, except for the compositional stability which is evaluated only after stressing the coatings in the climatic chamber. The evaluated parameters and their score values are listed in Table 4.

Table 4. Evaluation parameters and their score value for each coating (0 for unsatisfying results and 3 for well-performing outcomes).

Evaluation Parameters	Chitosan Gel	Proconsol®	Paraloid B72®
Compositional stability	2	3	2
Morphology	3	3	0
Color variance	2	2	1
Gloss variance	3	3	0
Hydrophobicity	2	0	3
Water vapor permeability (δp)	3	0 (n.a.)	2

Figure 8 shows the radar charts of the three products presented in this study: the bigger the area, the better-performing the product. Proconsol® presents very appealing performances in terms of morphology, color, gloss, and compositional stability; however, the doubts about the use of a $CaCO_3$-based material finally came up: the product, which is sold as a protective-consolidant material, does not present any hydrophobicity, hence the score attributed to the water vapor permeability is set to zero. Nevertheless, Proconsol® obtains a larger area than the still commonly-used Paraloid B72®, which excels in making the surface hydrophobic, presenting also passing permeability (δp) and chemical stability results; however, it fails in the aesthetic tests: color, gloss, and morphology variations, already visible before the artificial ageing, are far too evident to be ignored. On the other hand, the newly-proposed chitosan gel with AgNPs, even if does not show outstanding

results, is high-performing in most of the evaluation parameters, especially because it simultaneously offers both aesthetic stability and a compromise between hydrophobicity and water vapor permeability.
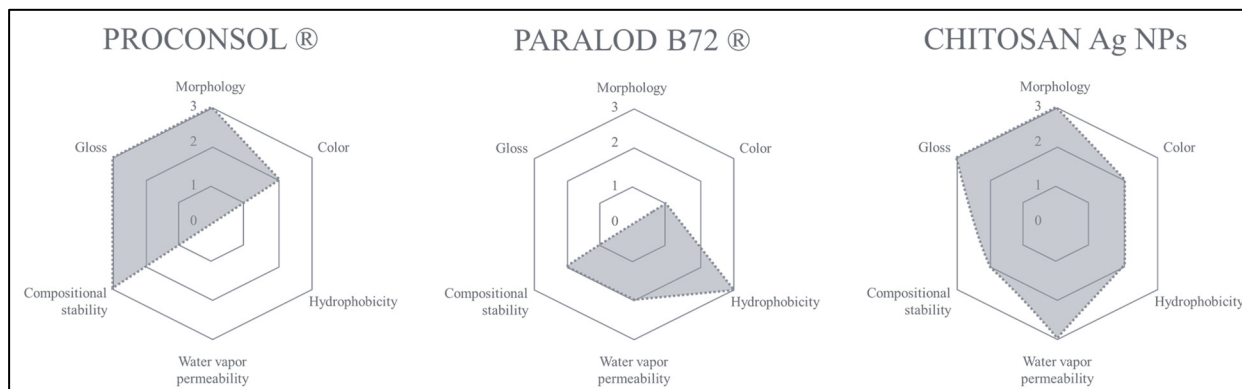

Figure 8. Radar charts used to evaluate the overall performance of the investigated coatings.

Thus, it can be said that the new formulation with chitosan and silver nanoparticles represents a valid alternative to the existing commercial products on the market today, proving to be effective and safe.

4. Conclusions

This work presented the formulation and characterization of a new product for outdoor frescoes protection, introducing the novelty of the synthesis method: nucleation and growth of silver nanoparticles in bio-polymer-based matrixes provides several chemical routes for organic-inorganic hybrid coating preparation. An enhanced control of particles growth seems to be provided by the stabilizing effect of bio-polymer-based gel introduced in the reaction with the double function of reducing, and capping and stabilizing agent. The controlled growth in shape and size of the silver nanoparticles is due to the azelaic and lactic acids solubilizing chitosan and obtaining the hosting gel matrix. Furthermore, the calcium hydroxide, as a precipitating agent, guarantees compatibility with the treated surface. Additional properties, such as a good transparency, hydrophobicity, intrinsic reversibility, and antimicrobial activity, are obtained by an adequate choice of the biopolymer and the inorganic nanoparticles type. Chitosan and silver nanoparticles emerge to produce an effective combination to obtain the desired properties for frescoes protection: the nanoparticles added to the coating base act on the surface roughness at the nanoscale, resulting in an increased hydrophobicity and consequent protection from water decay mechanisms.

The presented one-pot synthesis allows for obtaining a zero-waste formulation starting from non-toxic reagents, thus providing a new environment-friendly approach to the formulation of products designed for the conservation of Cultural Heritage. The one-pot method facilitates the optimization of reagents, avoiding product loss and assuring high homogeneity of the final product.

The application of the chitosan-based coating on fresco replicas was overall successful. Nanoparticles do not penetrate the surface layer of the *intonachino* and have been shown to endow the stratified system with hydrophobicity. This result strengthens the initial assumption that natural aging of frescoes can be strongly reduced by the application of hybrid coatings. The newly formulated coating shows good performances since it does not excessively alter surface morphology, has no gloss effects, and presents color variations lower than the human eye limit ($\Delta E = 2$). The interaction between water and the compound leads to an increase in surface hydrophobicity ($\theta = +51°$) without significantly altering the water vapor permeability (-12%). The artificial ageing does not affect the chemical stability of the synthesized product.

The comparison with the two traditional products for outdoor frescoes protection (ParaloidB72®and Proconsol®) shows the effectiveness of the Ag NPs-chitosan hybrid system in increasing the barrier properties of the treated samples, while keeping the external appearance unaltered. Proconsol does not confer hydrophobicity, leaving the surface sensitive to interaction with water; the ParaloidB72®, instead, creates a thicker shiny layer, limiting the water vapor permeability.

The encouraging results obtained represent the initial step toward new and extensive research on in situ frescoes protection. The next planned steps will be aimed to improve the overall performance of the coating, dealing with the optimization of the formulation to reduce the color variations and to further increase the hydrophobicity. Furthermore, although chitosan, azelaic acid, and AgNPs have documented antimicrobial properties, these compounds will be studied in relation to their interactions with microbiological colonization. Tests of natural ageing and of mechanical and thermal resistance will be conducted to obtain an overall evaluation of the performance of the formulation for subsequent commercial scale-up. Finally, the potential release rate of AgNPs into the environment, consequential to the leaching and/or degradation of the coating, will also be studied to complete the characterization of the material performances of the coating in outdoor environments.

References

1. Costantini, I.; Aramendia, J.; Tomasini, E.; Castro, K.; Manuel Madariaga, J.; Arana, G. Detection of Unexpected Copper Sulfate Decay Compounds on Late Gothic Mural Paintings: Assessing the Threat of Environmental Impact. *Microchem. J.* **2021**, *169*, 106542. [CrossRef]
2. Pérez-Diez, S.; Pitarch Martí, A.; Giakoumaki, A.; Prieto-Taboada, N.; Fdez-Ortiz de Vallejuelo, S.; Martellone, A.; De Nigris, B.; Osanna, M.; Madariaga, J.M.; Maguregui, M. When Red Turns Black: Influence of the 79 AD Volcanic Eruption and Burial Environment on the Blackening/Darkening of Pompeian Cinnabar. *Anal. Chem.* **2021**, *93*, 15870–15877. [CrossRef] [PubMed]
3. Sesana, E.; Gagnon, A.S.; Ciantelli, C.; Cassar, J.A.; Hughes, J.J. Climate Change Impacts on Cultural Heritage: A Literature Review. *Wiley Interdiscip. Rev. Clim. Chang.* **2021**, *12*, e710. [CrossRef]
4. Veneranda, M.; Prieto-Taboada, N.; de Vallejuelo, S.F.O.; Maguregui, M.; Morillas, H.; Marcaida, I.; Castro, K.; Madariaga, J.M.; Osanna, M. Biodeterioration of Pompeian Mural Paintings: Fungal Colonization Favoured by the Presence of Volcanic Material Residues. *Environ. Sci. Pollut. Res.* **2017**, *24*, 19599–19608. [CrossRef] [PubMed]

5. Morena, S.; Bordese, F.; Caliano, E.; Freda, S.; De Feo, E.; Barba, S. Architectural Survey Techniques for Degradation Diagnostics. an Application for the Cultural Heritage. *Int. Arch. Photogramm. Remote Sens. Spat. Inf. Sci.—ISPRS Arch.* **2021**, *46*, 449–454. [CrossRef]

6. Unković, N.; Dimkić, I.; Stupar, M.; Stanković, S.; Vukojević, J.; Grbić, M.L. Biodegradative Potential of Fungal Isolates from Sacral Ambient: In Vitro Study as Risk Assessment Implication for the Conservation of Wall Paintings. *PLoS ONE* **2018**, *13*, e0190922. [CrossRef]

7. Mang, S.M.; Scrano, L.; Camele, I. Preliminary Studies on Fungal Contamination of Two Rupestrian Churches from Matera (Southern Italy). *Sustainability* **2020**, *12*, 6988. [CrossRef]

8. De Luca, D.; Caputo, P.; Perfetto, T.; Cennamo, P. Characterisation of Environmental Biofilms Colonising Wall Paintings of the Fornelle Cave in the Archaeological Site of Cales. *Int. J. Environ. Res. Public Health* **2021**, *18*, 8048. [CrossRef]

9. Randazzo, L.; Montana, G.; Alduina, R.; Quatrini, P.; Tsantini, E.; Salemi, B. Flos Tectorii Degradation of Mortars: An Example of Synergistic Action between Soluble Salts and Biodeteriogens. *J. Cult. Herit.* **2015**, *16*, 838–847. [CrossRef]

10. Pérez, M.C.; García-Diego, F.J.; Merello, P.; D'Antoni, P.; Fernández-Navajas, A.; Ribera I Lacomba, A.; Ferrazza, L.; Pérez-Miralles, J.; Baró, J.L.; Merce, P.; et al. Pinturas Murales de La Casa de Ariadna (Pompeya, Italia): Un Estudio Multidisciplinar de Su Estado Actual Enfocado a Una Futura Restauración y Conservación Preventiva. *Mater. Constr.* **2013**, *63*, 449–467. [CrossRef]

11. Wollner, J.L. Planning Preservation In Pompeii: Revising Wall Painting Conservation Method and Management. *Stud. Mediterr. Antiq. Class.* **2013**, *3*, 5.

12. D'Andrea, A.; DI Lillo, A.; Laino, A.; Pesaresi, P.M. Documenting Large Archaeological Sites, Managing Data, Planning Conservation and Maintenance: The Herculaneum Conservation Project Experience. *Int. Arch. Photogramm. Remote Sens. Spat. Inf. Sci.—ISPRS Arch.* **2019**, *42*, 359–364. [CrossRef]

13. Matteini, M.; Mazzeo, R.; Moles, A. *Chemistry for Restoration: Painting and Restoration Materials*; Nardini Editore: Florence, Italy, 2016; p. 343.

14. Available online: https://www.cimminocalce.com/ (accessed on 12 May 2022).

15. Vaz, M.F.; Pires, J.; Carvalho, A.P. Effect of the Impregnation Treatment with Paraloid B-72 on the Properties of Old Portuguese Ceramic Tiles. *J. Cult. Herit.* **2008**, *9*, 269–276. [CrossRef]

16. Commentary on the ICOM-CC Resolution on Terminology for Conservation. The Working Method Note about the Task Force. In Proceedings of the 15th Triennial Conference, New Delhi, India, 22–26 September 2008.

17. Brandi, C. *Il Restauro. Teoria e Pratica (1939–1986)*; Saagi Arte, Editori Riuniti: Rome, Italy, 2009.

18. Artesani, A.; Di Turo, F.; Zucchelli, M.; Traviglia, A. Recent Advances in Protective Coatings for Cultural. *Coatings* **2020**, *10*, 217. [CrossRef]

19. Andreotti, S.; Franzoni, E.; Fabbri, P.; Fabbri, P. Poly(Hydroxyalkanoate)s-Based Hydrophobic Coatings for the Protection of Stone in Cultural Heritage. *Materials* **2018**, *11*, 165. [CrossRef]

20. Ocak, Y.; Sofuoglu, A.; Tihminlioglu, F.; Böke, H. Protection of Marble Surfaces by Using Biodegradable Polymers as Coating Agent. *Prog. Org. Coatings* **2009**, *66*, 213–220. [CrossRef]

21. Infurna, G.; Cavallaro, G.; Lazzara, G.; Milioto, S.; Dintcheva, N.T. Bionanocomposite Films Containing Halloysite Nanotubes and Natural Antioxidants with Enhanced Performance and Durability as Promising Materials for Cultural Heritage Protection. *Polymers* **2020**, *12*, 1973. [CrossRef]

22. Ivanov, V.; Stabnikov, V. *Basic Concepts on Biopolymers and Biotechnological Admixtures for Eco-Efficient Construction Materials*; Elsevier Ltd.: Amsterdam, The Netherlands, 2016; ISBN 9780081002148.

23. Giuliani, C.; Pascucci, M.; Riccucci, C.; Messina, E.; Salzano de Luna, M.; Lavorgna, M.; Ingo, G.M.; Di Carlo, G. Chitosan-Based Coatings for Corrosion Protection of Copper-Based Alloys: A Promising More Sustainable Approach for Cultural Heritage Applications. *Prog. Org. Coatings* **2018**, *122*, 138–146. [CrossRef]

24. Silva da Conceição, D.K.; Nunes de Almeida, K.; Nhuch, E.; Raucci, M.G.; Santillo, C.; Salzano de Luna, M.; Ambrosio, L.; Lavorgna, M.; Giuliani, C.; Di Carlo, G.; et al. The Synergistic Effect of an Imidazolium Salt and Benzotriazole on the Protection of Bronze Surfaces with Chitosan-Based Coatings. *Herit. Sci.* **2020**, *8*, 40. [CrossRef]

25. Trang, T.T.C.; Takaomi, K. Chitosan and Its Biomass Composites in Application for Water Treatment. *Curr. Opin. Green Sustain. Chem.* **2021**, *29*, 100429. [CrossRef]

26. Goy, R.C.; De Britto, D.; Assis, O.B.G. A Review of the Antimicrobial Activity of Chitosan. *Polimeros* **2009**, *19*, 241–247. [CrossRef]

27. Sanpui, P.; Murugadoss, A.; Prasad, P.V.D.; Ghosh, S.S.; Chattopadhyay, A. The Antibacterial Properties of a Novel Chitosan-Ag-Nanoparticle Composite. *Int. J. Food Microbiol.* **2008**, *124*, 142–146. [CrossRef] [PubMed]

28. Wang, X.; Hu, Y.; Zhang, Z.; Zhang, B. The Application of Thymol-Loaded Chitosan Nanoparticles to Control the Biodeterioration of Cultural Heritage Sites. *J. Cult. Herit.* **2022**, *53*, 206–211. [CrossRef]

29. Indrie, L.; Bonet-Aracil, M.; Ilieș, D.C.; Albu, A.V.; Ilieș, G.; Herman, G.V.; Baias, Ș.; Costea, M. Heritage Ethnographic Objects—Antimicrobial Effects of Chitosan Treatment. *Ind. Text.* **2021**, *72*, 284–288. [CrossRef]

30. Kim, J.S.; Kuk, E.; Yu, K.N.; Kim, J.H.; Park, S.J.; Lee, H.J.; Kim, S.H.; Park, Y.K.; Park, Y.H.; Hwang, C.Y.; et al. Antimicrobial Effects of Silver Nanoparticles. *Nanomed. Nanotechnol. Biol. Med.* **2007**, *3*, 95–101. [CrossRef]

31. Wang, C.; Sun, M.; Wang, H.; Zhao, G. Cubic Halide Double Perovskite Nanocrystals with Anisotropic Free Excitons and Self-Trapped Exciton Photoluminescence. *J. Phys. Chem. Lett.* **2023**, *14*, 164–169. [CrossRef]

32. Wang, Y.; Wang, Y.; Aravind, I.; Cai, Z.; Shen, L.; Zhang, B.; Wang, B.; Chen, J.; Zhao, B.; Shi, H.; et al. In Situ Investigation of Ultrafast Dynamics of Hot Electron-Driven Photocatalysis in Plasmon-Resonant Grating Structures. *J. Am. Chem. Soc.* **2022**, *144*, 3517–3526. [CrossRef]

33. Hasebe, S.; Hagiwara, Y.; Komiya, J.; Ryu, M.; Fujisawa, H.; Morikawa, J.; Katayama, T.; Yamanaka, D.; Furube, A.; Sato, H.; et al. Photothermally Driven High-Speed Crystal Actuation and Its Simulation. *J. Am. Chem. Soc.* **2021**, *143*, 8866–8877. [CrossRef]

34. Mokrzycki, W.S.; Tatol, M. Colour Difference ΔE—A Survey Mokrzycki. *Mach. Graph. Vis.* **2011**, *20*, 383–411.

35. Cimino, D.; Lamuraglia, R.; Saccani, I.; Berzioli, M.; Izzo, F.C. Assessing the (In)Stability of Urban Art Paints: From Real Case Studies to Laboratory Investigations of Degradation Processes and Preservation Possibilities. *Heritage* **2022**, *5*, 581–609. [CrossRef]

36. Costantini, R.; Vanden Berghe, I.; Izzo, F.C. New Insights into the Fading Problems of Safflower Red Dyed Textiles through a HPLC-PDA and Colorimetric Study. *J. Cult. Herit.* **2019**, *38*, 37–45. [CrossRef]

37. Striova, J.; Camaiti, M.; Castellucci, E.M.; Sansonetti, A. Chemical, Morphological and Chromatic Behavior of Mural Paintings under Er:YAG Laser Irradiation. *Appl. Phys.* **2011**, *104*, 649–660. [CrossRef]

38. UNI EN 15802:2010. Available online: http://store.uni.com/catalogo/uni-en-15802-2010?josso_back_to=http://store.uni.com/josso-security-check.php&josso_cmd=login_optional&josso_partnerapp_host=store.uni.com (accessed on 12 May 2022).

39. UNI EN 15803:2010. Available online: http://store.uni.com/catalogo/uni-en-15803-2010 (accessed on 12 May 2022).

40. Boanić, D.K.; Trandafilović, L.V.; Luyt, A.S.; Djoković, V. "Green" Synthesis and Optical Properties of Silver-Chitosan Complexes and Nanocomposites. *React. Funct. Polym.* **2010**, *70*, 869–873. [CrossRef]

41. Nishimura, S.; Mott, D.; Takagaki, A.; Maenosono, S.; Ebitani, K. Role of Base in the Formation of Silver Nanoparticles Synthesized Using Sodium Acrylate as a Dual Reducing and Encapsulating Agent. *Phys. Chem. Chem. Phys.* **2011**, *13*, 9335–9343. [CrossRef]

42. Berlangieri, C.; Poggi, G.; Murgia, S.; Monduzzi, M.; Dei, L.; Carretti, E. Structural, Rheological and Dynamics Insights of Hydroxypropyl Guar Gel-like Systems. *Colloids Surfaces B Biointerfaces* **2018**, *168*, 178–186. [CrossRef]

43. Farhadi Khouzani, M.; Chevrier, D.M.; Güttlein, P.; Hauser, K.; Zhang, P.; Hedin, N.; Gebauer, D. Disordered Amorphous Calcium Carbonate from Direct Precipitation. *CrystEngComm* **2015**, *17*, 4842–4849. [CrossRef]

44. Sanjuan, B.; Girard, J. Review of kinetic data on carbonate mineral precipitation. *Tetrahedron* **1996**, *52*, 13837–13866.

45. Hussein Elsayed, N.; Najmi, A.H.; Mohamed, G.M.; Mohamed, A.A.; Al-Sayed, H.M.A. Preparation and Characterization of Paraloid B-72/TiO$_2$ Nanocomposite and Their Effect on the Properties of Polylactic Acid as Strawberry Coating Agents. *J. Food Saf.* **2020**, *40*, e12838. [CrossRef]

46. Ciccola, A.; Serafini, I.; Guiso, M.; Ripanti, F.; Domenici, F.; Sciubba, F.; Postorino, P.; Bianco, A. Spectroscopy for Contemporary Art: Discovering the Effect of Synthetic Organic Pigments on UVB Degradation of Acrylic Binder. *Polym. Degrad. Stab.* **2019**, *159*, 224–228. [CrossRef]

47. Pintus, V.; Wei, S.; Schreiner, M. UV Ageing Studies: Evaluation of Lightfastness Declarations of Commercial Acrylic Paints. *Anal. Bioanal. Chem.* **2012**, *402*, 1567–1584. [CrossRef]

48. Papliaka, Z.E.; Andrikopoulos, K.S.; Varella, E.A. Study of the Stability of a Series of Synthetic Colorants Applied with Styrene-Acrylic Copolymer, Widely Used in Contemporary Paintings, Concerning the Effects of Accelerated Ageing. *J. Cult. Herit.* **2010**, *11*, 381–391. [CrossRef]

49. Shanti, R.; Bella, F.; Salim, Y.S.; Chee, S.Y.; Ramesh, S.; Ramesh, K. Poly(Methyl Methacrylate-Co-Butyl Acrylate-Co-Acrylic Acid): Physico-Chemical Characterization and Targeted Dye Sensitized Solar Cell Application. *Mater. Des.* **2016**, *108*, 560–569. [CrossRef]

50. Hammoude, A.Y.; Obeida, S.M.; Abboushi, E.K.; Mahmou, A.M. FT-IR Spectroscopy for the Detection of Diethylene Glycol (DEG) Contaminant in Glycerin-Based Pharmaceutical Products and Food Supplements. *Acta Chim. Slov.* **2020**, *67*, 530–536. [CrossRef]

51. Joshi, R.; Joshi, R.; Amanah, H.Z.; Faqeerzada, M.A.; Jayapal, P.K.; Kim, G.; Baek, I.; Park, E.-S.; Masithoh, R.E.; Cho, B.-K. Quantitative Analysis of Glycerol Concentration in Red Wine Using Fourier Transform Infrared Spectroscopy and Chemometrics Analysis. *Korean J. Agric. Sci.* **2021**, *48*, 299–310.

52. Debandi, M.V.; Bernal, C.; Francois, N.J. Development of Biodegradable Films Based on Chitosan/Glycerol Blends Suitable for Biomedical Applications. *J. Tissue Sci. Eng.* **2016**, *7*, 3. [CrossRef]

53. Leceta, I.; Peñalba, M.; Arana, P.; Guerrero, P.; De La Caba, K. Ageing of Chitosan Films: Effect of Storage Time on Structure and Optical, Barrier and Mechanical Properties. *Eur. Polym. J.* **2015**, *66*, 170–179. [CrossRef]

54. Bussiere, P.O.; Gardette, J.L.; Rapp, G.; Masson, C.; Therias, S. New Insights into the Mechanism of Photodegradation of Chitosan. *Carbohydr. Polym.* **2021**, *259*, 117715. [CrossRef] [PubMed]

55. Pino, F.; Fermo, P.; La Russa, M.; Ruffolo, S.; Comite, V.; Baghdachi, J.; Pecchioni, E.; Fratini, F.; Cappelletti, G. Advanced Mortar Coatings for Cultural Heritage Protection. Durability towards Prolonged UV and Outdoor Exposure. *Environ. Sci. Pollut. Res.* **2017**, *24*, 12608–12617. [CrossRef]